Journal of Materials Processing Technology 213 (2013) 913–925

Contents lists available at SciVerse ScienceDirect

Journal of Materials Processing Technology

journal homepage: www.elsevier.com/locate/jmatprotec

The manufacturing and replication of microfluidic mould inserts by the hot embossing process

M. Sahli*, C. Millot, J.-C. Gelin, T. Barrière

FEMTO-ST Institute, Applied Mechanics Department, CNRS UMR 6174, ENSMM, 25030 Besançon Cedex, France

ARTICLE INFO

Article history:
Received 6 May 2012
Received in revised form 1 November 2012
Accepted 5 November 2012
Available online 14 November 2012

Keywords:
Hot embossing
Copper powders
Feedstock
Binders
Rheology
Sintering

ABSTRACT

In this paper, the manufacturing of metallic microfluidic mould inserts is studied based on the hot embossing process. The feedstocks are prepared and analysed. The quality of the feedstock resulting from the mixing process is found to depend on numerous parameters, such as the mixing time, the mixing temperature, the shear rate and the powder loading. The present mixing study is conducted with copper powders. The thermal and rheological properties of the selected feedstock under various mixing conditions are determined and used to establish the necessary conditions for mixing, hot embossing and debinding to obtain the copper microfluidic mould inserts. Sintering at different temperatures is conducted under vacuum. The effects of the sintering temperatures are evaluated based on the sintered microstructures. In this work, the dimensional variations in the microfluidic samples, in particular the dimensional shrinkage, global warpage and surface roughness at each stage of the process, are quantified and compared in detail.

1. Introduction

Micromanufacturing of metallic cavity die moulds for micro-injection moulding or hot embossing of micro-structured components can be realised through several different processes. For example, the required patterns can be obtained using through mechanical manufacturing processes for material removal. The performance of this method, which accomplishes material removal by micro-milling, leads to the formation of burrs; hence, the machined parts require further processing, and the burrs cannot always be completely eliminated. To avoid these structuring complications, a new processing strategy for the manufacturing of mould die cavities has been investigated and developed. Photolithography, micro-casting, mixing, hot embossing, debinding and solid state sintering stages have been sequentially combined to process cavity die moulds, which have been further characterised by surface roughness measurements.

Becker and Heim (2000) described the process as a very versatile replication method that can be used to duplicate the structured cavities from the master into the material. The process enables the possibility to obtain micro-structures with sizes ranging from several micrometres to only a few micrometres in range with high accuracy and high quality based on the application of elevated temperatures and high contact forces to the polymeric components. Heckele et al. (1998) reported that this process is actually used only for a few optical applications in which high precision and high quality are important. The approach involves heating a polymer plate to its softening temperature (i.e., just above the glass transition temperature for an amorphous thermoplastic polymer) and then pressing it in a mould with an applied pressure. The polymer is cooled down, and then the component is de-moulded at room temperature. The process offers many important advantages, such as cost efficiency, accuracy, proper reproducibility and fast development of complex shapes, great flexibility in material choice and relatively fast time cycles with a significant reduction in cost compared to the conventional polymer processing techniques.

Many studies have investigated the hot embossing process in recent years. Lin et al. (2003) investigated the pressure distributions on the polymer surface during the hot embossing process. The results indicated that the quality of a product manufactured by hot embossing is affected by its shrinkage during cooling. Therefore, the shrinkage of a polymer depends on the embossing pressure. Sahli et al. (2009) investigated and compared the replication quality of polymeric replicas obtained by filling microcavities. The results provided information on the reliability concerning the possibility of replicating topographical surface geometries using both hot embossing and micro-injection moulding processes. Heyderman et al. (2000) studied the viscous flow of thin PMMA films into microcavities during hot embossing. Two fill mechanisms were observed, including the simple flow of PMMA from the borders and the formation of polymer mounds. Li et al. (2008) carried out a series of experiments to investigate the processing of micro-components

* Corresponding author. Tel.: +33 381666040; fax: +33 381402852.
E-mail address: Mohamed.sahli@ens2m.fr (M. Sahli).

0924-0136/$ – see front matter © 2012 Elsevier B.V. All rights reserved.
http://dx.doi.org/10.1016/j.jmatprotec.2012.11.007

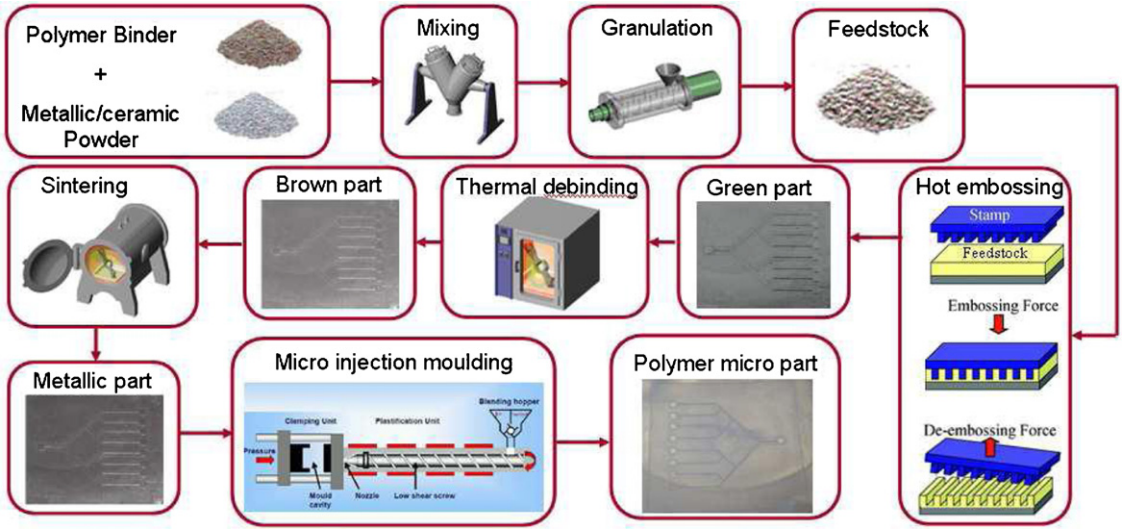

Fig. 1. A schematic illustration of the multistage sequential manufacturing process used for micro-structured die mould inserts, combining the hot embossing process and powder metallurgy processes.

by hot embossing. The results of their research identified that the replication accuracy strongly depends on the processing conditions and on the processing temperature and pressure in particular.

In the present analysis, the hot embossing process was used to obtain metallic cavity die moulds at a lower cost than the conventional processes can achieve in relation to manufacturing or micro-machining processes. The proposed approach combines the hot embossing process and related powder metallurgy processes. This approach was developed for the rapid manufacturing of high quality metallic replicas on elastomeric moulds, as illustrated in Fig. 1. In this process, the metallic powders are mixed with a polymeric binder system, which mainly includes thermoplastic polymers. The resulting mixture is called feedstock and is then embossed in the mould to achieve the required shapes. After, the binder is removed during thermal debinding, and the powder is sintered, yielding the full density necessary to give the required mechanical properties and geometry size, within the same time that a certain amount of shrinkage occurs.

In recent years, a significant number of investigations concerning the effects of processing parameters with respect to the powder loading of feedstocks have been carried out towards the development of powder injection technologies. However, the control of dimensional accuracy has received comparatively little attention. Considering the small dimensions used in this technology, the binder system must be appropriately selected to provide lower viscosity to easily fill the cavity die mould during injection moulding process, as reported by Liu et al. (2005). In this work, Liu et al. (2005) also investigated the effects of the melt temperature, mould temperature and packing pressure on the filling, microstructure replication and de-moulding aspects of the procedure. The results demonstrated that 316 L stainless steel microstructures can be successfully replicated through the μPIM route.

Liu et al. (2001) focused on establishing a suitable binder system for μPIM. They found that a reduction in the PW content, as well an increase in either HDPE or EVA, allows an increase in the green strength of the parts, which enables easier part handling. Their results also demonstrated enhanced shape retention during debinding. The findings indicate that 316 L stainless steel microparts can be moulded, debound and sintered successfully using a suitable binder system. Heaney and Spina (2007) investigated predictions of the shrinkage of a metal injected moulded component using numerical simulations. The results obtained are capable of settling the shrinkage problems in metal injection moulding (MIM) and correcting the designs in injection moulding. Srivatsan et al. (2002) performed an investigation of the influence of powder particle sizes on the resulting microstructures, including the presence and distribution of the porosity, cracks, density and micro-hardness of tungsten carbide pieces. Three different particle sizes were chosen and used to make the tungsten carbide samples. The results reveal that pulsing of the powders prior to consolidation lead to higher density and micro-hardness values in comparison to those obtained by consolidating the powders without pulse conditions. Moballegh et al. (2005) studied powder processing to obtain copper components by means of metal injection moulding technology. They observed that injection moulding of a feedstock loaded with copper powder up to 60% could be accomplished only at low pressures. The resulting sintered components are free from defects, and the dimensional shrinkages were found to be nearly the same in all three dimensions. The related results were used to understand the importance of an appropriately selected binder system in the achievement of lower viscosity for easy filling of mould cavities during the hot embossing process, as well as proper shape retention and dimensional changes during the debinding and sintering stages without distortion, warpage or cracking for the resulting embossed components.

Liu et al. (2005) investigated the mixing, characterisation and feasibility of an in-house feedstock for the injection moulding of microstructures. They studied and analysed the effects of powder loading and extrusion on mixing and feedstock homogeneity. The results showed that it is possible to successfully manufacture the microstructures with good shape retention using feedstock comprised of 316 L stainless steel and a multi-component binder system. Meng et al. (2011) used MIM injection moulding to fabricate the micro-parts. The results showed that microstructures can be successfully fabricated without visual defects and with good shape retention. It has been found that the grain believes significantly with increasing sintering temperatures, and thus it led to a decrease in the micro-hardness. Tay et al. (2006) successfully replicated two sets of 316 L stainless steel micro-rod arrays using the micro-metal injection moulding process (μMIM). Proper shape retention was attained for the sintered components without distortion, warpage or cracking. After sintering, the shrinkage in the micro-rods was nearly isotropic with very similar microhardness values measured on the polished cross-sections of the micro rod arrays. Additionally, reduced porosity was also observed on the micro-rod structures achieved. Lahiri and Bhargava (2009)

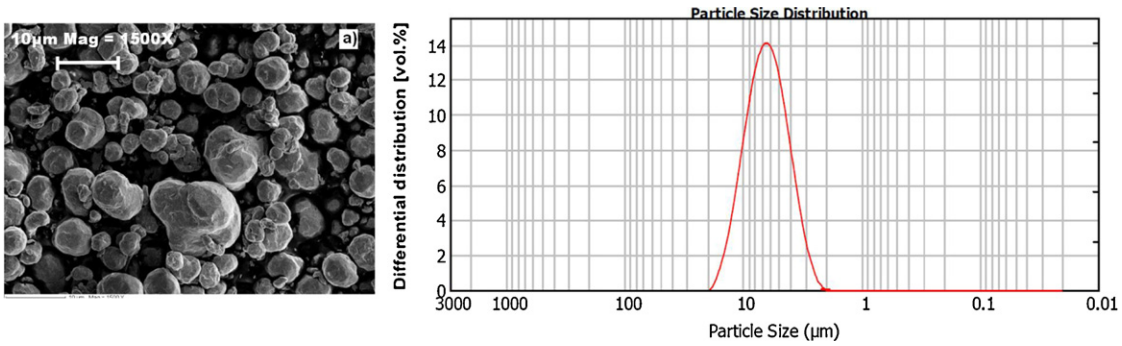

Fig. 2. (a) A scanning electron micrograph of the copper powder and (b) a particle size distribution for the copper powder (d_{50} = 6.34 μm).

studied the compaction and sintering process with mechanically alloyed Cu–Cr powders. They concluded that the explosive compaction of mechanically alloyed Cu–Cr powder followed by the solid-state sintering or coating of mechanical powder with Cu followed by uni-axial cold compaction and solid-state sintering could be a better option for the production of electrical contact materials. Moreover, many factors were also found to control the final porosity of the components during the elaboration of porous copper compacts using the powder metallurgy process. The filler material amount and its type, sintering temperature, sintering time and the compaction pressure have been recognised as the most important parameters, as reported by Ahmed et al. (2007). Leong and Liu (1997) have used copper powder with an average size of 63 μm after mixing to obtain a paste feedstock, which was compacted in a mould container to obtain rectangular specimens, then sintered at 800 °C and 1000 °C. The authors indicated that the advantage of these sintered wicks could be attributed to the existence of smaller pores with controlled porosity and pore size, optimising heat pipe performance. In this analysis, the possibility to replicate both the roughness and surface micro-shapes in metallic materials as required for the manufacturing of metallic masters were demonstrated through hot embossing, which can be used as cavity die moulds to transfer patterns on polymer substrates, e.g., in microfluidic applications. This paper covered the manufacturing of metallic microfluidic replicas using the hot embossing process. We studied the complete process of copper hot embossing with a developed binder system, based on polypropylene (PP), paraffin wax (PW) and stearic acid (SA). Different powder loadings were used in the study and a suitable powder loading was selected. In this study, the evolution of torque during the mixing step, the homogeneity and flow properties of the mixtures were studied. The mixing, hot embossing and debinding conditions were optimised, and finally, the sintering process was studied. The surface roughness was found to depend on the sintering temperature and affects the hardness of the microfluidic samples.

2. Materials and experimental procedures

2.1. Materials

The characteristics of the powders that were used in the present study are related in Table 1. The copper powders were provided by Eurotungsten Eramet® with average particles size d_{10} = 3.73 μm, d_{50} = 6.34 μm, and d_{90} = 10.81 μm and with a theoretical density equal to 8.92 g/cm^3. Typical scanning electron micrographs of the copper powder reveal the morphology, as shown in Fig. 2a. Fig. 2b gives a photograph of the copper powder particle distribution. The binder components used in this analysis included paraffin wax, stearic acid and polypropylene, all provided by Sigma–Aldrich®. The composition of the binder system used is related in Table 2.

Table 1
The main characteristics of the copper powder.

Chemical symbol	Cu
Particle shape	Irregular
Density (g/cm^3)	8.92
Tape density	4.63
Melting point (°C)	1084
Boiling point (°C)	2565
Thermal conductivity (W m^{-1} K^{-1})	401

2.2. Copper feedstock preparation

The experiments related to the mixing of binders and feedstocks were conducted using a twin screw Brabender® Plastograph EC mixer with a pair of rotor blades. This equipment has a chamber volume of 55 cm^3, and 73% of this volume was used for the tests. The mixing temperature was chosen according to the melting point of polypropylene (T_f = 125 °C) and below the degradation temperature of paraffin wax (T_d = 250 °C) as well as stearic acid (T_d = 180 °C). This allowed complete melting and prevented binder degradation.

Two different mixing tests were conducted to determine the proper mixing parameters, such as the mixing time, the shear rate, and the critical solid loading. (i) The first test consisted of an evaluation of the critical solid loading in the feedstock, using a continuously increasing powder loading fraction from 40% to 75%. During mixing, the binder system was fed into the mixer first, followed by the addition of powder in small consecutive loadings. (ii) The second test consisted of elaborated mixtures, which were determined on the basis of the critical value obtained. Generally, the feedstocks were loaded slightly lower than the critical value. The formulation used in this study was proposed by Quinard et al. (2009).

2.3. Thermal degradation properties and rheology characterisation

The degradation temperature ranges of the binder components in powder-binder feedstocks were obtained by thermogravimetric analysis (TGA). The analyses indicated the thermal limitations of the initial processes, including the mixing and soft embossing processes. TGA was carried out with a Setaram Setsys analyser® in the

Table 2
A summary of the thermo-physical properties of the binders.

Binder constituents	Type	Density (g/cm^3)	Melting temperature (°C)
Polypropylene (PP)	Secondary	0.90	125
Paraffin wax (PW)	Primary	0.91	60
Stearic acid (SA)	Surfactant	0.89	70

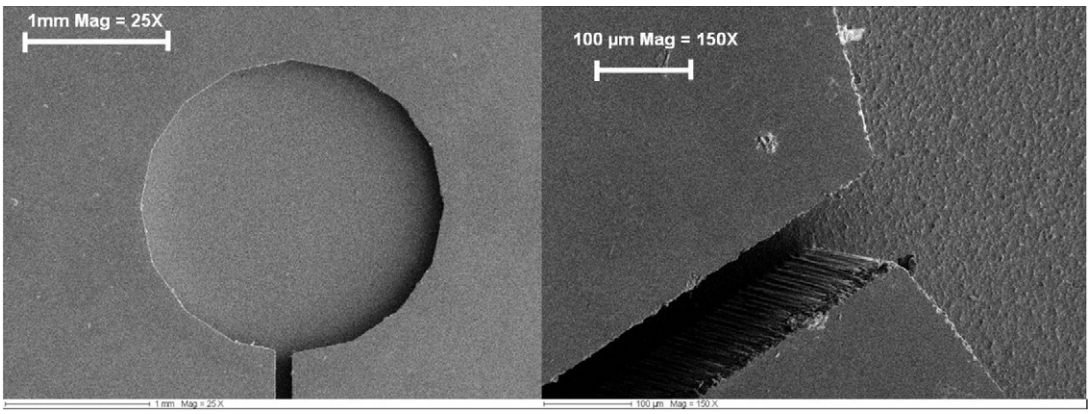

Fig. 3. SEM micrographs of the silicon die mould: (a) a micro-reservoir with a diameter and depth of 2000 and 100 μm, respectively and (b) a micro-channel with a width and depth of 100 and 100 μm, respectively.

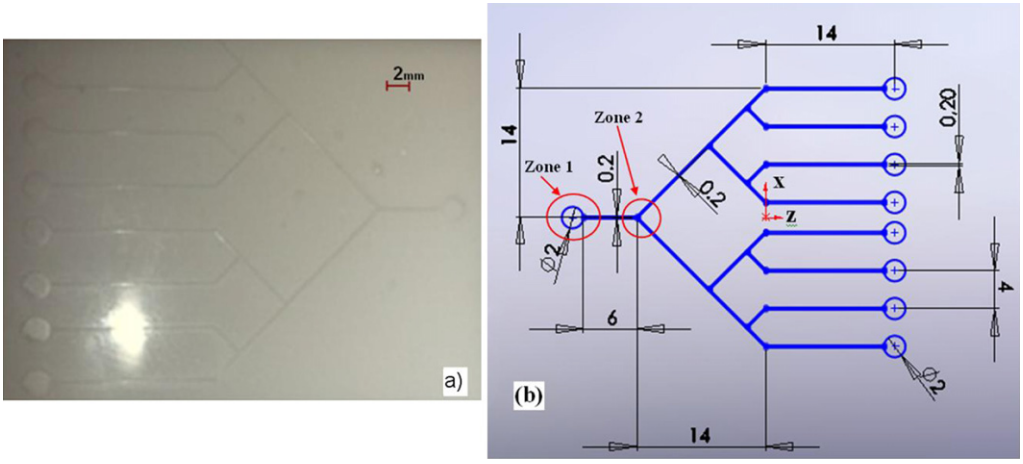

Fig. 4. (a) The pattern geometries of the elastomeric cavity die moulds and (b) a schematic of the microfluidic pattern (all units in mm).

presence of nitrogen atmosphere up to 500 °C at a heating rate of 5 °C/min.

The viscosity of the feedstocks was measured with a Bohlin® capillary rheometer. Ten minutes were allowed for each sample to reach thermal equilibrium, after loading the barrel and reaching the testing temperature. The feedstocks were extruded through a die with a diameter of 1 mm and a length of 16 mm. The test temperatures were 150, 160 and 170 °C beyond the melting temperature of the binder. The shear rate was chosen in the range from 10^2 to 10^4 s^{-1}, and a melting time of 10 min was employed for each test to reach thermal equilibrium after charging the barrel.

2.4. Si-die mould fabrication

The silicon (Si) mould master was manufactured with microfluidic structures by means of photolithography and the deep reactive ion etching technique (DRIE) to emboss microfluidic structures on the copper feedstocks (Fig. 3). The cavity die mould was manufactured as follows. First, the wafer was cleaned in piranha for 2 min, followed by rinsing with deionised water for 2 min and dehydration on a hot plate at 110 °C for 5 min. A 2.5-μm-thick SPR220-3.0 positive photoresist was deposited on the surface of the wafer using a spin coater at a spin speed of 1200 rpm and a spinning time of 30 s.

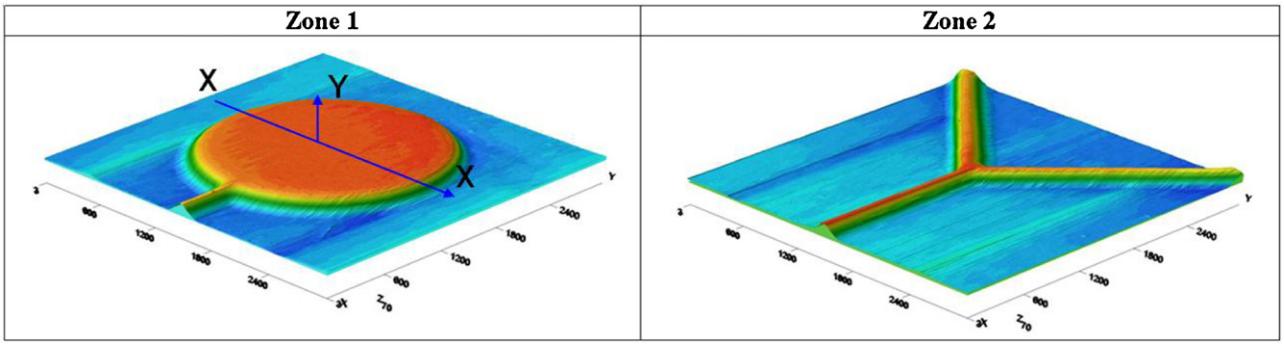

Fig. 5. Three-dimensional topographic imprints of the elastomeric cavity die moulds, as realised by casting of a RTV 3428.

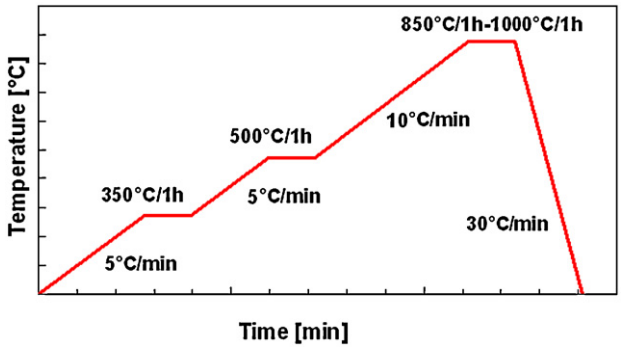

Fig. 6. The thermal debinding and sintering profiles.

The photoresist was then soft baked at 115 °C for 15 min on a hot plate, followed by cooling to room temperature.

The resist was exposed using an EVG620 aligner with an exposure energy of 300 mJ/cm^2. Deep reactive ion etching (DRIE) was performed on Alcatel A601 equipment with the Bosch process technology. Silicon structures were obtained with a depth of approximately 100 μm. Finally, the dies were treated with C4F8 passivation gas under a flow of 500 sccm for 5 min to create a thin layer of Teflon-like material on the sidewall surfaces to further facilitate the mould release and to reduce friction between the Si die mould and the elastomeric replicas during de-moulding. To determine the replication accuracy, the profile and dimensions of the micro-channels in the dies were compared with those in the embossed copper replicas.

2.5. Hot embossing process

The hot embossing tests were gradually carried out to an imposed test load (400 N) using a universal testing equipment (type 6025, Instron®). In this process, the forming temperature of both separately controlled rigid metallic platens may rise up to 300 °C. In the hot embossing tests, the elastomeric cavity die moulds used were realised by casting the liquid material over a Si master, which enables micro-structures to be obtained with well defined, smooth sidewalls with very low roughness values.

The silicone rubber (RTV 3428) provide by Bluestar Silicones® was used as the material for the elastomeric moulds. The silicone base and the catalyst were thoroughly mixed at a ratio eq. 10:1. The mixture was degassed during approximately 5 min in primary vacuum to avoid the trapping of air in the silicone, leading to a porous matrix and defects in the resulting replicas. Next, the mixture was poured over the Si die mould and cured at 70 °C over the course of 4 h. Fig. 4a shows micrographs of the patterned PDMS substrates used in this study. A schematic drawing detailing the dimensions of the micro-structures in the elastomeric mould is shown in Fig. 4b. The forming temperature of the proposed feedstock was tested in the range from 130 to 170 °C.

The dimensions, surface roughness and surface topography of the elastomeric mould insert and microfluidic samples were probed with a mechanical profilometer (Tencor-Alpha Step IQ) with a diamond tip measuring 5 μm in radius operated with a scanning speed of 5 μm/s over a length of 1 mm inside and outside the reservoir pattern of 2 mm in diameter on the elastomeric mould insert and the micro-system samples (zone 1, see Fig. 4b). The shrinkage of the microfluidic sample was determined based on the dimensional changes in the width and height of the micro-sized structure. Two detailed scans of the elastomeric cavity die mould shapes are illustrated in Fig. 5a and b, as obtained with SMM; these shapes were achieved by casting in two different zones.

2.6. Debinding and sintering stages

Two sequential stages must be considered here, including thermal debinding followed by solid state sintering. In the thermal debinding stage, the residual binders were converted into gas and eliminated. Then, the powder skeleton was sintered and consequently the green component was strengthened to prevent products without defects.

The thermal cycle kinetic profiles of the debinding stage used was based on TGA curves for the binder systems that lead to total weight loss of the binder. The samples were introduced in the furnace, and the temperature was gradually increased from 350 to 500 °C to remove any residual binder (see Figs. 6 and 7). The samples were maintained at this temperature for 1 h, and then sintering was carried out at several different sintering temperatures,

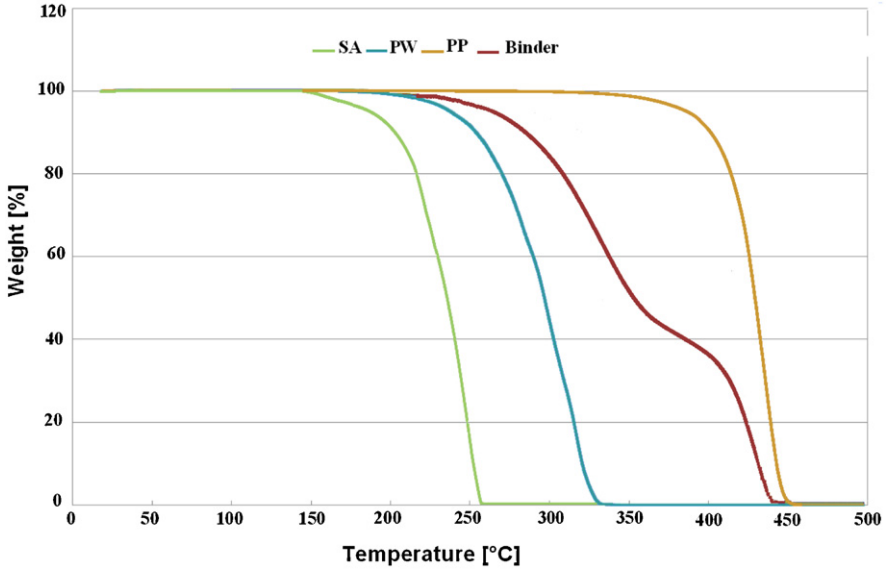

Fig. 7. The TGA analyses of the binder system.

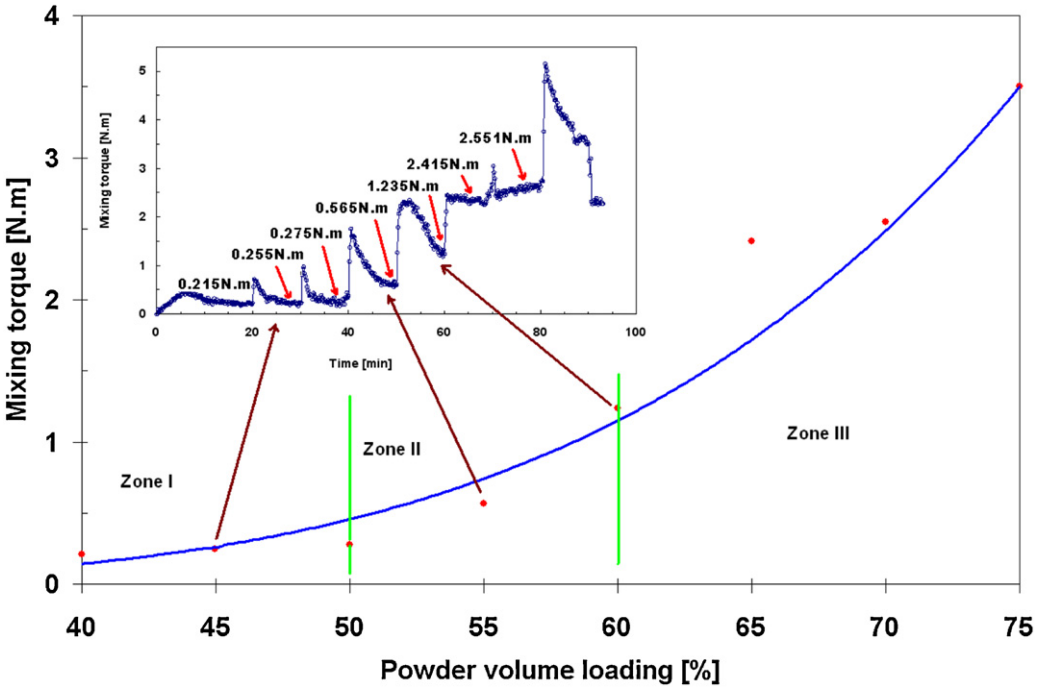

Fig. 8. The mixing torque vs. the powder volume loading obtained by continuously increasing the copper powder volume in the loading process during the mixing stage, obtained at 160 °C.

ranging from 850 to 1000 °C, with a temperature rate of 10 °C/min for copper (see Fig. 6).

3. Results and discussion

3.1. Thermal degradation characteristics

Thermogravimetric analysis (TGA) of the feedstock is essential for determining the maximum temperature of the embossing process and for removal of the binder during the thermal debinding cycle. Fig. 7 shows the weight loss with the temperature of the binder and the pure components, heated at 10 °C/min. The pure components decompose in one step. PW and SA start to decompose at 200 °C, and total evaporation occurs at approximately 400 °C. PP decomposition starts at approximately 420 °C and finishes at 500 °C. However, binder decomposition occurs in two stages. The first weight loss occurs between 200 and 400 °C, corresponding to the elimination of PW and SA. In the second step, degradation occurs more rapidly than in the first step, from 420 to 500 °C. Above 450 °C, all of the binder components have been burned off. Based on the TGA results, a multi-step debinding profile was established to demonstrate the progressive removal of the three binder components. The use of progressive debinding occurring over a wide temperature range can help to retain the integrity of the microstructures, further preventing the formation of debinding defects, such as cracking and slumping.

3.2. Preparation and characterisation of the feedstocks

For the first test, the powder loading was increased gradually from 40% to 75% by incremental powder addition of 5% per level. This methodology was also used in the past by Jardiel et al. (2008)

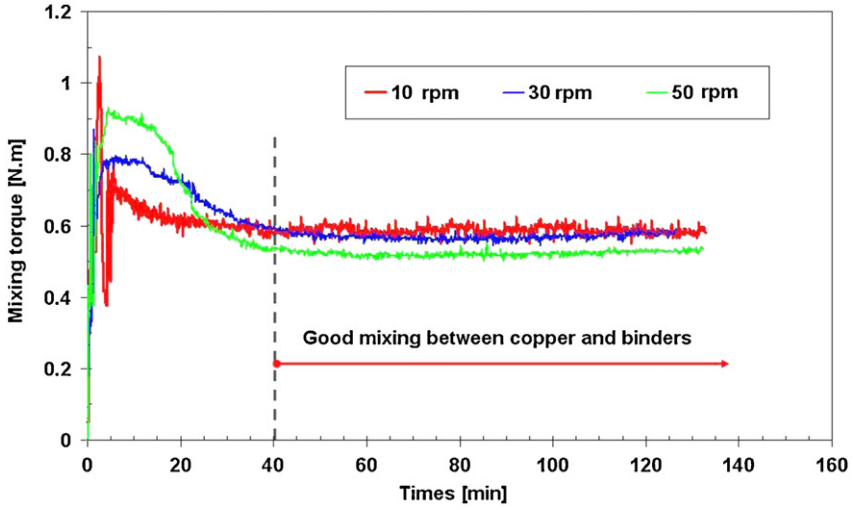

Fig. 9. The mixing torque vs. the mixing time profiles associated with the feedstocks containing 60 vol.% of copper, obtained at 160 °C with different mixing velocities.

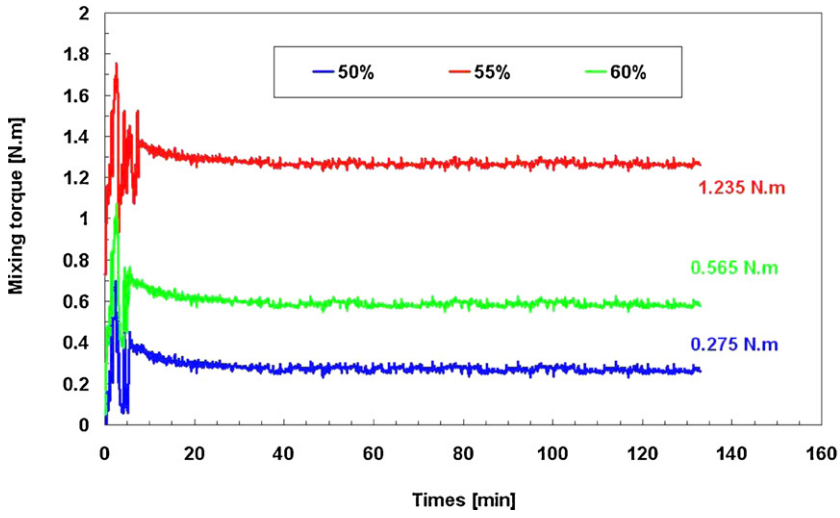

Fig. 10. The mixing torque vs. the mixing time profiles for several feedstock mixtures at different solid fractions.

to determine the critical solid volume loading. This test can provide a means for obtaining the critical solid volume loading in a simple following only one testing cycle. Jardiel et al. (2008) developed a new multi-component thermoplastic binder system for injection moulding. They also found that surface coating of the powder can reduce the viscosity of the feedstock without requiring high proportions of PW in the binder composition.

The final mixing torque is related in Fig. 8 as a function of the mixing time. Three different zones appear upon consideration of the curve presented in Fig. 8. In zone I, the mixture primarily contains binder, and the degree of torque remains low. In zone II (50–60%), the torque gradually increases with enhanced homogenisation. In zone III (65–75%), a very rapid increase in the mixing torque and associated torque values became too large for filling micro-cavities during the hot embossing process. The critical powder volume loading was determined to be equal to 65 vol.% (zone III). These measures enabled a determination of the range in loading rates, which is necessary to prepare homogeneous mixtures; all mixtures were prepared in the range of 50–60%.

Fig. 9 shows the variation in torque with time during the mixing experiments. The experiments were performed at a mixing temperature of 160 °C (according to the TGA tests) and at different rotation speeds from 10 at 50 rpm. It was observed that the torque increased slightly as the roller speed was increased from 10 to 30 rpm and then decreased thereafter. However, the roller speed appeared to have an insignificant effect on the feedstock properties. Additionally, significant homogenisation was observed when the processing time was longer than 40 min. These copper feedstocks were mixed at times less than 40 min, giving a high degree of heterogeneity. These measures led to a determination of the proper mixing conditions, and according to the TGA tests, the mixing temperature, rotation speed and mixing time were found to be 160 °C, 50 rpm and 40 min, respectively. The same findings were observed in both feedstocks, elaborated at solid loadings equal to 50% and 55%.

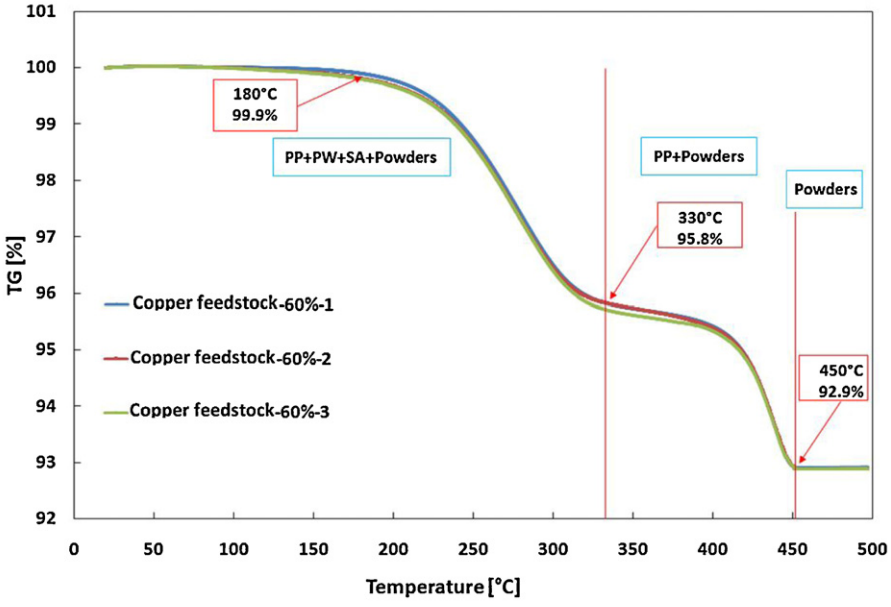

Fig. 11. TGA curves for the copper feedstock with a 60 vol.% solid loading.

For example, the experimental results related in Fig. 10 reveal the mixing behaviour of the feedstocks loaded between 50 to 60 vol.%, the total volumes of the copper powders. The mixing conditions already were determined and are described earlier in this study. The conditions indicate that the final mixing torque used for the copper powders corresponded to 50% loading percentages less than the others. The final mixing torque was approximately 0.275 Nm, which corresponded to 50 vol.% of powder loadings in comparison with 0.565 Nm and 1.235 Nm for powder volume loadings of 55 and 60 vol.%. Hence, it can be concluded that a powder volume loading equal in volume to 50% gives the lowest torque. In this study, a powder volume loading equal to 60% was chosen for the feedstock elaboration, which was determined to be necessary for replication by hot embossing.

The main goal of mixing is to produce a homogeneous feedstock with suitable rheological behaviour for the subsequent processing steps. The thermogravimetric results presented in Fig. 11 show that the mixed feedstock is more homogeneous because the corresponding thermogravimetric curves were replicated better than the feedstock. Additionally, the standard deviation of the binder losses for the mixed feedstock is 1.10×10^{-2} (wt.%). The feedstock homogeneity after the mixing stage was examined with scanning electron microscopy (Fig. 12).

3.3. Viscosity measurements and analysis

Fig. 13 shows the variation in apparent viscosity vs. the shear rate for different temperatures. This figure clearly demonstrates the rheological behaviour of the feedstocks, which can be considered non-Newtonian fluids. It was observed that lower viscosities were obtained for higher temperatures (corresponding to 170 °C). At a higher melting temperature, the feedstock exhibited lower viscosities that were highly suitable for the hot embossing process.

3.4. Hot embossing results

The experimental procedure was conducted at different temperatures from 130 to 170 °C in which 400 N was applied once the embossing temperature was reached. In Fig. 14, each view corresponds to the forming temperature stage (the forming process) used for the reservoirs and micro-channels. At 130 °C, which is close to the PP melting temperature, the surfaces of the embossed patterns were extremely rough, caused by partial melting of the binder system. However, the filling ratio increases with increasing forming temperature, leading to an accurate replica of the original imprint.

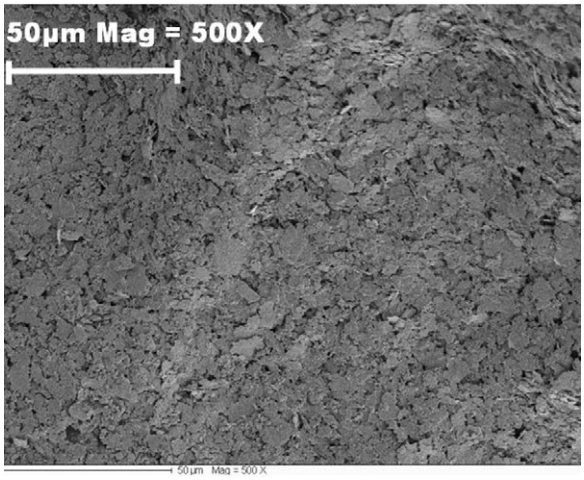

Fig. 12. An SEM photograph of the copper feedstock obtained after 40 min at 160 °C and 50 rpm with a solid loading equal to 60%.

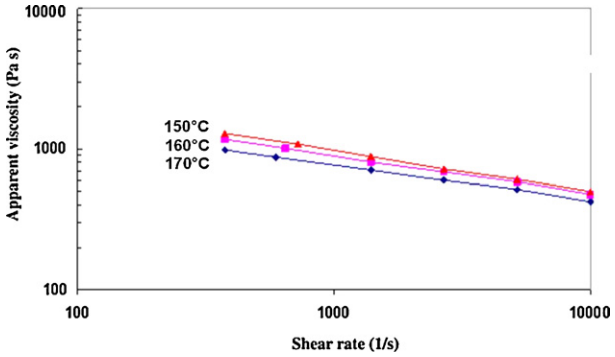

Fig. 13. The viscosity of the copper feedstock with a solid loading equal to 60 vol.% elaborated at different temperatures.

After several tests, it was found that the temperature strongly influenced the resulting filling rate and the final surface roughness of the cavities. For example, at 170 °C, the feedstocks were pushed by the binders towards the mould details, leaving fewer defects in the final shapes. The average surface roughness, R_a, measured at the base of the reservoirs, decreased sharply at the melting temperature, followed by a levelling off at higher temperatures (beyond 160 °C).

As an example, Fig. 15 shows the filling development of the micro-replication in comparison with the degree of forming temperature variation in the range from 150 to 170 °C. It was found that the filling ratio increase more significantly enhanced the accuracy of the replica in comparison with the original imprint mould with increasing forming temperature. The filling rate difference can be attributed to the rheological behaviour of the material. In conclusion, the temperature range used for the replications carried out with the hot embossing process can be limited to the range of 160 °C to 180 °C. A proper filling is obtained within this range. Beyond, the stearic acid begins to degrade.

3.5. Debinding and sintering results

Fig. 16 shows various debinding replicas obtained using feedstocks elaborated by different mixing times. A short mixing time was found to lead to non-uniform mixing feedstocks, which can impact the quality of replicas (e.g., leading to strong agglomeration, significant variations in feedstock homogeneity, etc.). This observation correlates to the mixing time used for the feedstock. The results show that the feedstock can be used for the successful manufacturing of the microstructures (with a mixing time $\geq$40 min). The same observations were observed for feedstocks containing 50–60 vol.% copper.

The sizes and dimensions of the sintered parts were measured and compared with the geometry of the embossed parts to analyse the shrinkage associated with the sintering stage. The analyses of the dimensions were carried out on the sintered specimens embossed with copper feedstocks loaded from 56% to 60%. The components undergo important dimensional isotropic shrinkage events in the range from 14% to 18% (see Figs. 17 and 18). This dimensional change occurs homogeneously across the sample, so it can be compensated in the design of the template.

Fig. 17 shows a photograph of the microfluidic components after undergoing different processing steps. On the one hand, analysis of the different microfluidic embossed samples shows that the use of a higher solid loading of feedstock improves the embossed sample rigidity with lower thermal stress after demoulding, which results in good global flatness after demoulding. On the other hand, micro embossing at the lowest temperature with acceptable fidelity

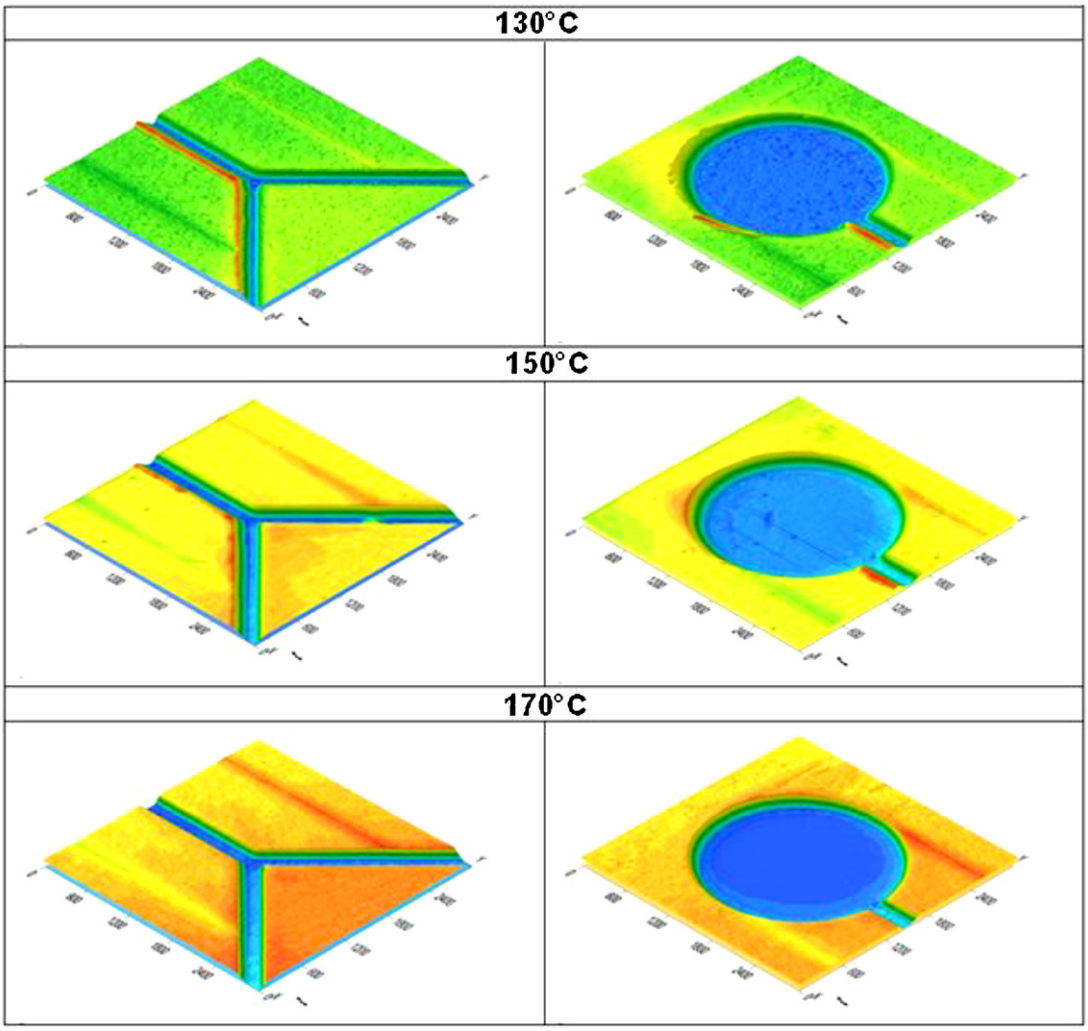

Fig. 14. 3D topographic metallic replications obtained with the hot embossing process using copper feedstocks with a solid loading equal to 60 vol.% at different forming temperatures.

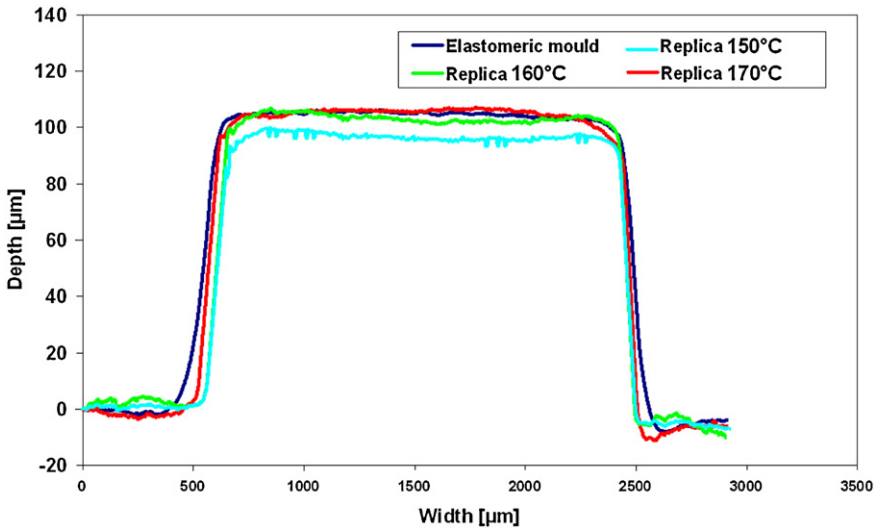

Fig. 15. A comparative variation in the 2D topographic profiles for the elastomeric moulds and the copper replicas obtained by hot embossing at different temperatures, along the *x*–*x* direction (zone 1).

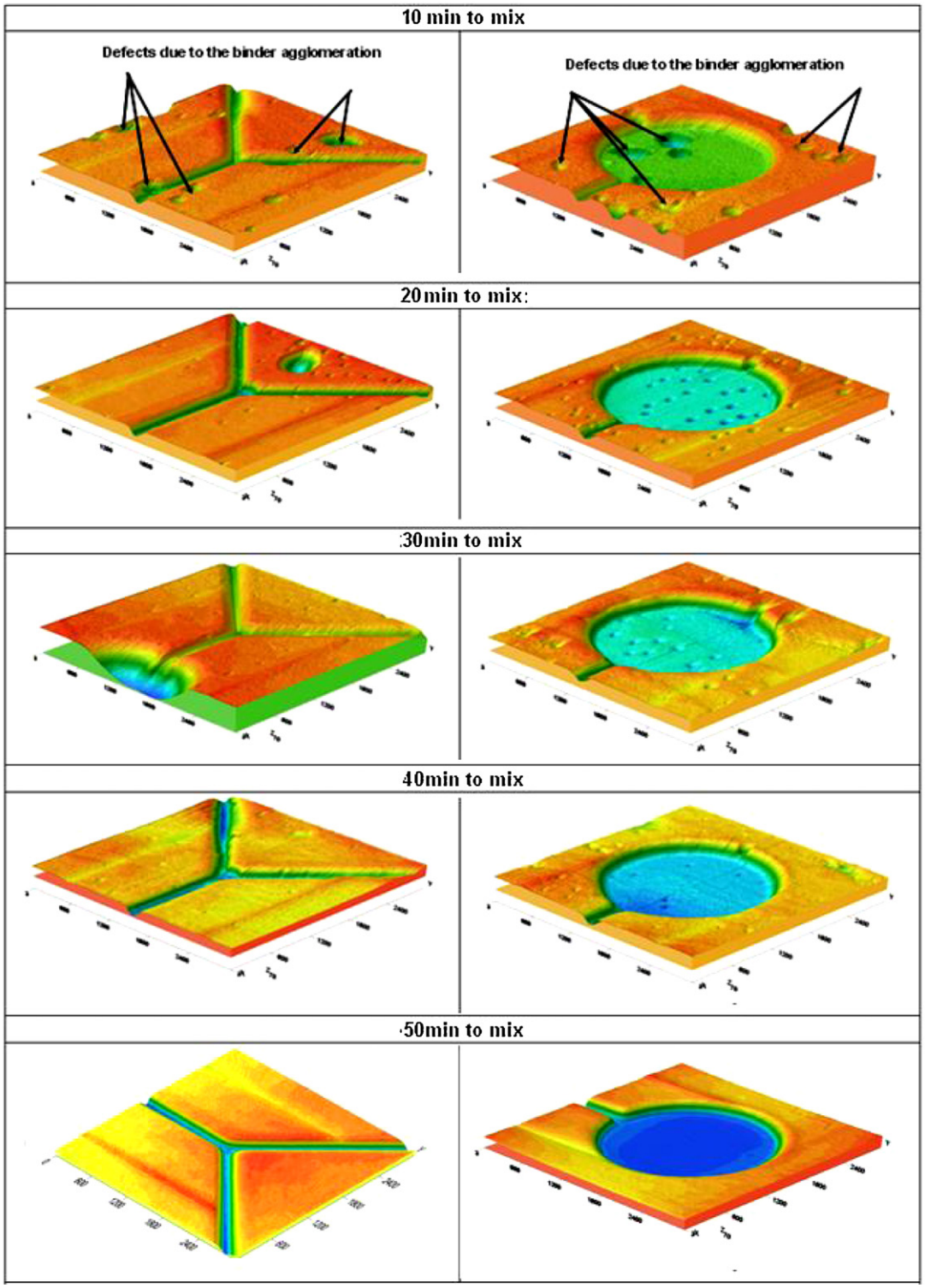

Fig. 16. 3D topographic images of copper replicas obtained by embossing at approximately 170 °C, followed by debinding at a temperature up to 350 °C, using different feedstocks, which were obtained from different mixing times (the feedstocks contained 60 vol.% copper).

can improve the global flatness after demoulding. Comparing the sintered microstructures and the embossed microstructures, it can be observed that the shape retention of the sintered microstructures has been successfully realised. No visual defects can be observed on the sintered component. In comparison with the embossed component, dimensional changes after debinding are not noticeable, although the dimensional changes after sintering may be clearly evident.

The dimensions of the elastomeric mould insert, following both embossing and sintering of the microfluidic parts, were measured with a confocal profiler. Measurements were conducted at six different locations on the microfluidic part, as shown in Fig. 18. The dimensions of the microfluidic structures at different solid loadings are shown in Tables 3 and 4. In comparison with the elastomeric mould insert, the dimensional changes after the sintering stage are clearly evident. The dimensional changes in

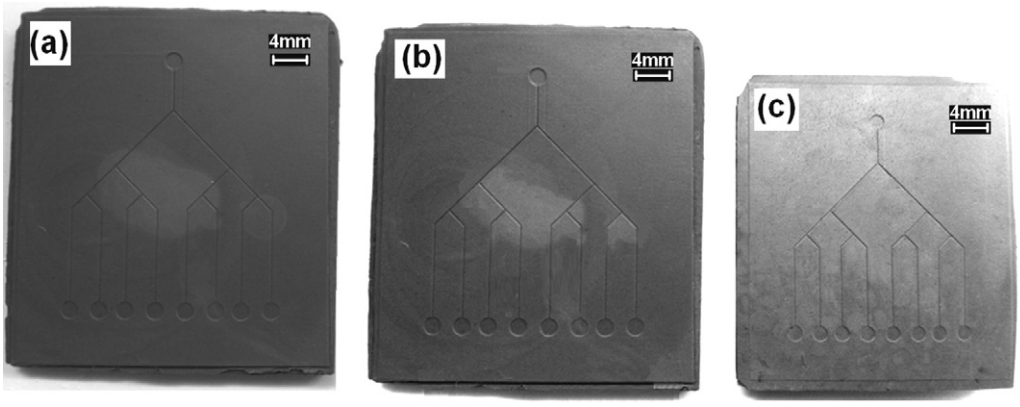

Fig. 17. Photographs of the microfluidic replicas after different processing steps: (a) embossed to 170 °C, (b) dedinded up to 350 °C and (c) sintered up to 1000 °C.

Table 3
Shrinkage in the *y*–*y* direction corresponding to the microfluidic structure in zone 1 (with a sintering time of 60 min).

Shrinkage in depth direction (*y*–*y*)	Solid loading								
	56%	58%	60%	56%	58%	60%	56%	58%	60%
Sintering temperature		800 °C			900 °C			1000 °C	
Heating rate					10 (°C/min)				
	15.9	15.3	14.7	16.3	15.8	15.1	17.8	16.2	15.6

Table 4
Dimensions of the elastomeric insert mould and micro-sized structure of the microfluidic samples sintered at 1000 °C.

Dimensions (mm)	Elastomeric mould insert	Micro-sized structure		
		56%	58%	60%
Ø	2	1.65 ± 0.01	1.67 ± 0.01	1.69 ± 0.01
a	6	4.92 ± 0.01	5.03 ± 0.01	5.10 ± 0.01
b	14	11.54 ± 0.01	11.72 ± 0.01	11.80 ± 0.01
c	14	11.51 ± 0.02	11.70 ± 0.02	11.82 ± 0.02
d	4	3.29 ± 0.01	3.36 ± 0.01	3.37 ± 0.01
e	14	11.48 ± 0.02	11.73 ± 0.02	11.77 ± 0.02

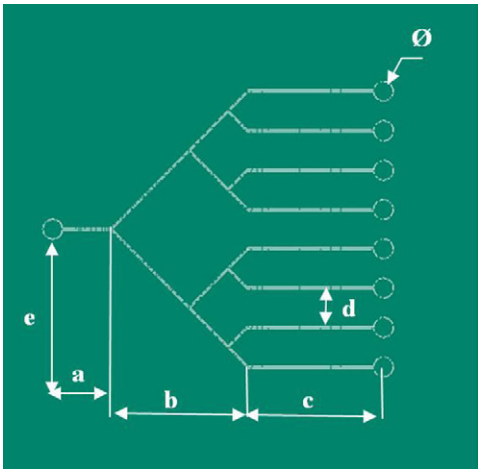

Fig. 18. A cross section of the locations of the dimensional measurements gathered from the microfluidic part.

the length and width dimensions of the micro-structures showed similar trends. However, the width and height of the embossed micro-structures decreased gradually as the sintering temperature increased (Fig. 19).

The effects of debinding and the sintering temperature on the surface roughness of the sintered components, as reflected by the R_a gap between the different phases of component sintering process of sintered components, are shown in Fig. 20. Roughness measurements were conducted on components sintered at different temperatures. These values were compared with the measurement values made on the elastomeric mould. It can be observed that increasing the sintering temperature causes a slight increase in the surface roughness of the materials, accompanied by a slight rounding of the ends and corners at temperatures beyond to 1000 °C.

Additionally, the density of the sintered copper replicas were measured by hydrostatic weighing, according to the evaluated sintering temperature. The hydrostatic density was determined based on the ratio between the mass of the component in air and its mass in a fluid (pure ethanol). It was observed that, by increasing the sintering temperature from 900 to 1000 °C, the density increased from 8.0 to 8.3 g/cm^3. The density increase in this temperature range was only 2%. The observed density eq. 8.3 g/cm^3 was found to be approximately 93% of the theoretical density. However, the proposed processing manner has the ability to attain over 97% of the theoretical density. Hence, to achieve a higher density of the sintered components, some of the processing conditions should be optimised.

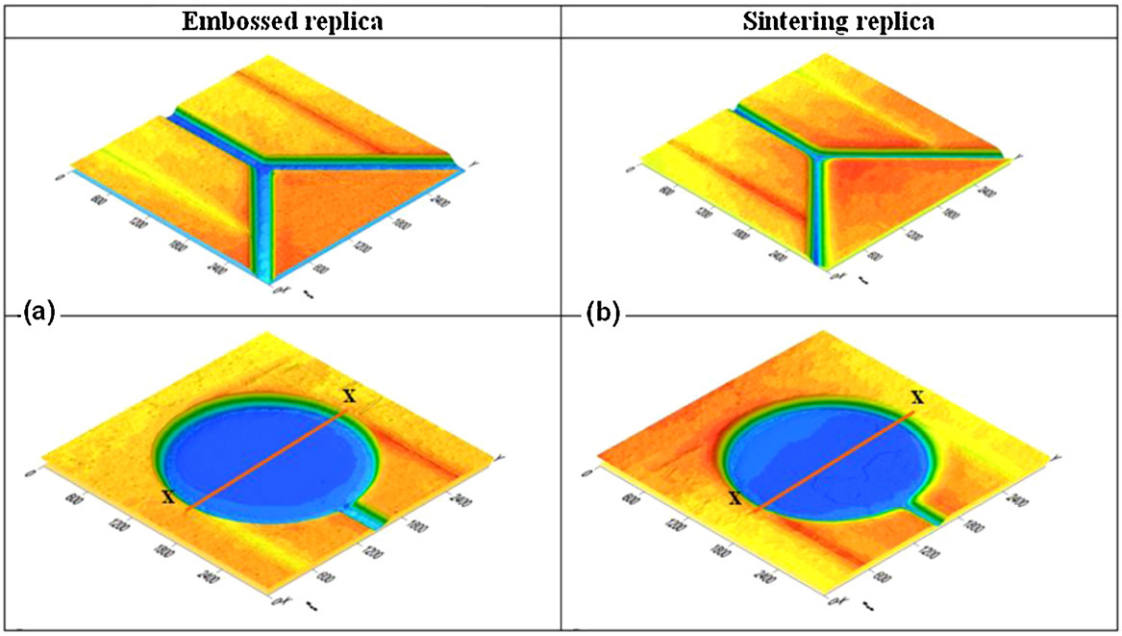

Fig. 19. 3D topographic images of the copper replicas obtained after different processing steps: (a) hot embossing at 170 °C and (b) after sintering up to 1000 °C.

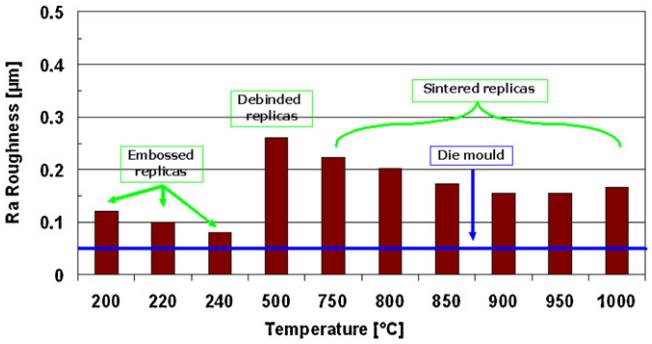

Fig. 20. Evolution of the surface roughness of the copper replicas after different processing steps.

4. Conclusions

In this study, the possibility to replicate both roughness details and surface micro-shapes in elastomeric masters, as needed for the manufacturing of metallic die moulds, was demonstrated. These metallic replicas will be used later as die cavity moulds to transfer the patterns onto polymer substrates, e.g., for microfluidic applications. This paper relates the technological approach and the scientific achievements related to the imprinting of metallic substrates by using hot embossing. The manufacturing strategy combines several processing sequences, which are mainly based on combinations of the hot embossing process, polymer debinding and solid-state diffusion in the sintering stages. These combinations were carefully investigated.

For the copper powder and binder components used, a suitable powder loading of 60 vol.% was established based on the application of a steady-state mixing torque, augmented by suitable rheological characteristics. The latter analysis enabled the establishment of suitable processing conditions for the hot embossing and debinding stages related to a copper micro-component. We showed the studied feedstock potential by taking into account the complete process, from feedstock preparation to sintering, then through embossing and debinding. Debinding was performed thermally. Finally, after optimising the thermal cycle of the sintering step, we successfully obtained samples with microfluidic details that had good shape retention without visible defects, such as warpage, incomplete filling or cracking. The dimensions of the micro-channel components changed with variations in the processing steps. Moreover, the experimental results confirm that the components exhibit homogeneous shrinkage after debinding and sintering in the range from 14 to 18% for the mixtures under consideration. High densification was achieved at 1000 °C.

References

Ahmed, Y.M.Z., Riad, M.I., Sayed, A.S., Ahlam, M.K., Shalabi, M.E.H., 2007. Correlation between factors controlling preparation of porous copper via sintering technique using experimental design. Powder Technology 175, 48–54.
Becker, H., Heim, U., 2000. Hot embossing as a method for the fabrication of polymer high aspect ratio structures. Sensors and Actuators 83, 130–135.
Heaney, D.F., Spina, R., 2007. Numerical analysis of debinding and sintering of MIM parts. Journal of Materials Processing Technology 191, 385–390.
Heckele, M., Bacher, W., Müller, K.D., 1998. Hot embossing – the moulding technique for plastic microstructures. Microsystem Technologies 4, 122–124.
Heyderman, L.J., Schift, H., David, D., 2000. Flow behaviour of thin polymer films used for hot embossing lithography. Microelectronic Engineering 54, 229–245.
Jardiel, T., Sotomayor, M.E., Levenfeld, B., Várez, A., 2008. Optimization of the processing of 8-YSZ powder by powder injection molding for SOFC electrolytes. International Journal of Applied Ceramic Technology 5 (6), 574–581.
Lahiri, I., Bhargava, S., 2009. Compaction and sintering response of mechanically alloyed Cu–Cr powder. Powder Technology 189, 433–438.
Leong, K.C., Liu, C.Y., 1997. Characterization of sintered copper wicks used in heat pipes. Journal of Porous Materials 4, 303–308.
Li, J.M., Liu, C., Peng, J., 2008. Effect of hot embossing process parameters on polymer flow and microchannel accuracy produced without vacuum. Journal of Materials Processing Technology 207, 163–171.
Lin, C.R., Chen, R.H., Hung, C., 2003. Preventing non-uniform shrinkage in open die hot embossing of PMMA micro-structures. Journal of Materials Processing Technology 140, 173–178.
Liu, L., Loh, N.H., Tay, B.Y., Tor, S.B., Khor, K.A., Murakoshi, Y., 2005. Mixing and characterization of 316 L stainless steel feedstock to micro powder injection molding. Materials Characterization 54, 230–238.
Liu, Z.Y., Loh, N.H., Tor, S.B., Khor, K.A., Murakoshi, Y., Maeda, R., 2001. Binder system for micropowder injection molding. Materials Letters 48, 31–38.
Meng, J., Loh, N.H., Fu, G., Tay, B.Y., Tor, S.B., 2011. Micro powder injection moulding of alumina micro-channel part. Journal of the European Ceramic Society 31, 1049–1056.

Moballegh, L., Morshedian, J., Esfandeh, M., 2005. Copper injection moulding using a thermoplastic binder based on paraffin wax. Materials Letters 59, 2832–2837.
Quinard, C., Barrière, T., Gelin, J.C., 2009. Development and property identification of 316L stainless steel feedstock for PIM and μPIM. Powder Technology 190, 123–128.
Sahli, M., Millot, C., Roques-Carmes, C., Khan Malek, C., Gelin, J.C., Barrière, T., 2009. Quality assessment of polymer replication by hot embossing and micro-injection molding processes using Scanning Mechanical. Microscopy Journal of Materials Processing Technology, 5851–5861.
Srivatsan, T.S., Woods, R., Petraroli, M., Sudarshan, T.S., 2002. An investigation of the influence of powder particle size on microstructure and hardness of bulk samples of tungsten carbide. Powder Technology 122, 54–60.
Tay, B.Y., Liu, L., Loh, N.H., Tor, S.B., Murakoshi, Y., Maeda, R., 2006. Characterization of metallic micro rod arrays fabricated by μMIM. Materials Characterization 57, 80–85.